Efficient calculation of interior scattering from cavities with partial IBC wall

Xinlei Chen✉, Xiuqiang Liu, Zhuo Li and Changqing Gu

The magnetic field integral equation based method of moments (MoM) with the Kirchhoff approximation can predict the interior scattering from cavities with impedance boundary condition (IBC) walls. However, if the IBC wall is a small part of the whole wall and is modified multiple times, the conventional MoM may be time-consuming due to the repeated and expensive lower–upper (LU) decompositions of impedance matrices. In this Letter, the Sherman–Morrison–Woodbury (SMW) formula is used to mitigate the problem. The authors only require to perform the LU decomposition of the cavity without IBC walls, and to efficiently obtain the solutions of the cavity with different IBC walls by reusing the LU decomposition and the SMW formula.

Introduction: The prediction of the interior scattering from open-ended cavities is an important aspect in designing stealthy engine inlets and nozzles. Previous research [1–3] shows that the magnetic field integral equation (MFIE) with the Kirchhoff approximation (KA) [1, 4] can be used to calculate the interior scattering from cavities. To solve the MFIE, the iterative physical optics (IPO) [1] and the method of moments (MoM) [2, 3] can be applied. However, the MoM can give more accurate results than the IPO for complex cavities [2]. If the cavity wall is imperfectly conducting or coated with thin dielectric sheet, the impedance boundary condition (IBC) [5] model can be employed [6, 7]. In practice, the IBC wall may be a relatively small part of cavity wall, and its area and surface impedance may be repeatedly modified to realise better radar cross section (RCS) reduction. However, the conventional MoM [2] is time-consuming for this type of application because of the repeated solutions of matrix equations. In this Letter, the Sherman–Morrison–Woodbury (SMW) formula-based technique [8–10] is applied to circumvent this problem.

Formulations: As shown in Fig. 1, a cavity with partial IBC wall illuminated by a plane wave $\left(\boldsymbol{E}^i, \boldsymbol{H}^i\right)$ is considered. The equivalent electric current $\boldsymbol{J}(\boldsymbol{r})$ and magnetic current $\boldsymbol{M}(\boldsymbol{r})$ on the cavity's interior walls S_c satisfy the MFIE as follows [6, 7]:

$$\hat{\boldsymbol{n}}(\boldsymbol{r}) \times \boldsymbol{H}_a^i(\boldsymbol{r}) = \frac{\boldsymbol{J}(\boldsymbol{r})}{2} - \hat{\boldsymbol{n}}(\boldsymbol{r}) \times \text{P.V.}\int_{S_c} \boldsymbol{J}(\boldsymbol{r}') \times \nabla G(\boldsymbol{r}, \boldsymbol{r}')\text{d}s' + \frac{\text{j}k}{\eta}\hat{\boldsymbol{n}}(\boldsymbol{r}) \times \int_{S_b} \bar{\boldsymbol{G}}(\boldsymbol{r}, \boldsymbol{r}') \cdot \boldsymbol{M}(\boldsymbol{r}')\text{d}s' \tag{1}$$

where k, η, G and $\bar{\boldsymbol{G}}$ are the wavenumber, impedance, Green's function and dyadic Green's function in free space, respectively. The unit normal vector $\hat{\boldsymbol{n}}(\boldsymbol{r})$ points into the cavity. P.V.$\int$ denotes the principal value of the integral. $\boldsymbol{M}(\boldsymbol{r})$ and $\boldsymbol{J}(\boldsymbol{r})$ on the IBC wall S_b satisfy the relationship

$$\boldsymbol{M}(\boldsymbol{r}) = -\hat{\boldsymbol{n}}(\boldsymbol{r}) \times \eta_r \eta \boldsymbol{J}(\boldsymbol{r}) \tag{2}$$

where η_r is the normalised surface impedance.

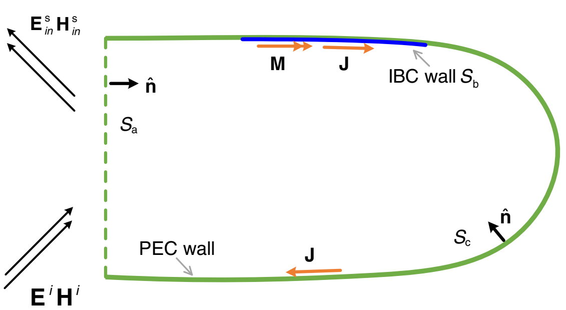

Fig. 1 *Cavity with partial IBC wall is illuminated by plane wave*

In order to estimate the interior scattering from the cavity, the incident magnetic field $\boldsymbol{H}_a^i(\boldsymbol{r})$ on S_c is evaluated by the KA [1, 4] as

$$\boldsymbol{H}_a^i(\boldsymbol{r}) \simeq -\int_{S_a} \boldsymbol{J}^i(\boldsymbol{r}') \times \nabla G(\boldsymbol{r}, \boldsymbol{r}')\text{d}s' - \frac{\text{j}k}{\eta}\int_{S_a} \bar{\boldsymbol{G}}(\boldsymbol{r}, \boldsymbol{r}') \cdot \boldsymbol{M}^i(\boldsymbol{r}')\text{d}s' \tag{3}$$

where $\boldsymbol{J}^i(\boldsymbol{r}) = \hat{\boldsymbol{n}}(\boldsymbol{r}) \times \boldsymbol{H}^i(\boldsymbol{r})$ and $\boldsymbol{M}^i(\boldsymbol{r}) = \boldsymbol{E}^i(\boldsymbol{r}) \times \hat{\boldsymbol{n}}(\boldsymbol{r})$ are the equivalent electric and magnetic current induced by the incident plane wave.

In order to solve (1) and (2), the RWG basis functions are used to expand $\boldsymbol{J}(\boldsymbol{r})$ and $\boldsymbol{M}(\boldsymbol{r})$ [11]

$$\boldsymbol{J}(\boldsymbol{r}) = \sum_{n=1}^{N} I_n \boldsymbol{f}_n(\boldsymbol{r}), \ \boldsymbol{M}(\boldsymbol{r}) = \eta \sum_{n=1}^{N_{\text{ibc}}} P_n \boldsymbol{g}_n(\boldsymbol{r}). \tag{4}$$

where N and N_{ibc} are the numbers of RWG for expanding $\boldsymbol{J}(\boldsymbol{r})$ and $\boldsymbol{M}(\boldsymbol{r})$, respectively. And $N_{\text{ibc}} \ll N$, because we assume the IBC wall is a small part of the whole cavity wall.

Then, (1) and (2) are discretised by the MoM into the matrix equations

$$\boldsymbol{ZI} + \boldsymbol{CP} = \boldsymbol{V} \tag{5}$$

$$\boldsymbol{DP} = \boldsymbol{RI} \tag{6}$$

where $\boldsymbol{I}$ and $\boldsymbol{P}$ include the unknown coefficients. The sizes of $\boldsymbol{Z}$, $\boldsymbol{C}$, $\boldsymbol{D}$ and $\boldsymbol{R}$ are $N \times N$, $N \times N_{\text{ibc}}$, $N_{\text{ibc}} \times N_{\text{ibc}}$ and $N_{\text{ibc}} \times N$, respectively. The elements in $\boldsymbol{Z}$, $\boldsymbol{C}$, $\boldsymbol{D}$ and $\boldsymbol{R}$ are

$$Z_{mn} = \frac{1}{2}\int \boldsymbol{f}_m(\boldsymbol{r}) \cdot \boldsymbol{f}_n(\boldsymbol{r})\text{d}s - \int \boldsymbol{f}_m(\boldsymbol{r}) \times \hat{\boldsymbol{n}}(\boldsymbol{r}) \cdot \text{P.V.}\int \nabla G(\boldsymbol{r}, \boldsymbol{r}') \times \boldsymbol{f}_n(\boldsymbol{r}')\text{d}s'\text{d}s \tag{7}$$

$$C_{mn} = \text{j}k \int \boldsymbol{f}_m(\boldsymbol{r}) \times \hat{\boldsymbol{n}}(\boldsymbol{r}) \cdot \int \bar{\boldsymbol{G}}(\boldsymbol{r}, \boldsymbol{r}') \cdot \boldsymbol{g}_n(\boldsymbol{r}')\text{d}s'\text{d}s \tag{8}$$

$$D_{mn} = \int \boldsymbol{g}_m(\boldsymbol{r}) \cdot \boldsymbol{g}_n(\boldsymbol{r})\text{d}s \tag{9}$$

$$R_{mn} = -\int \eta_r(\boldsymbol{r})\boldsymbol{g}_m(\boldsymbol{r}) \cdot \hat{\boldsymbol{n}}(\boldsymbol{r}) \times \boldsymbol{f}_n(\boldsymbol{r})\text{d}s \tag{10}$$

we can compute $\boldsymbol{I}$ before $\boldsymbol{P}$ and the solutions of (5) and (6) are

$$\boldsymbol{I} = \left(\boldsymbol{Z} + \boldsymbol{CD}^{-1}\boldsymbol{R}\right)^{-1}\boldsymbol{V} \tag{11}$$

$$\boldsymbol{P} = \boldsymbol{D}^{-1}\boldsymbol{RI} \tag{12}$$

It can be found that the lower–upper (LU) decomposition of $\boldsymbol{Z} + \boldsymbol{CD}^{-1}\boldsymbol{R}$ has to be performed each time the area or the surface impedance of the IBC wall is modified. Thus, the conventional MoM is time-consuming for such application. In this Letter, the SMW formula [8–10] is employed to address this problem. According to the SMW formula [10], (11) can be rewritten as

$$\boldsymbol{I} = \left(\boldsymbol{Z}^{-1}\boldsymbol{V}\right) - \left(\boldsymbol{Z}^{-1}\boldsymbol{C}\right)\left(\boldsymbol{D} + \boldsymbol{RZ}^{-1}\boldsymbol{C}\right)^{-1}\boldsymbol{R}\left(\boldsymbol{Z}^{-1}\boldsymbol{V}\right) \tag{13}$$

it can be seen that the LU decompositions of $\boldsymbol{Z}$ and $\boldsymbol{D} + \boldsymbol{RZ}^{-1}\boldsymbol{C}$ need to be computed. Although the size of $\boldsymbol{Z}$ is the same as the size of $\boldsymbol{Z} + \boldsymbol{CD}^{-1}\boldsymbol{R}$, the LU decomposition of $\boldsymbol{Z}$ needs to be calculated only once and can be reused for different IBC walls. Furthermore, the size of $\boldsymbol{D} + \boldsymbol{RZ}^{-1}\boldsymbol{C}$ is much smaller than the size of $\boldsymbol{Z} + \boldsymbol{CD}^{-1}\boldsymbol{R}$, because $N_{\text{ibc}} \ll N$. Thus, (13) is much more efficient than (11) when the IBC wall is modified multiple times.

After the wall electric and magnetic current is found, as done in [1, 2], the KA [1, 4] is applied again to estimate the RCS contributed by the cavity interior scattering

$$\boldsymbol{E}_{\text{in}}^s(\boldsymbol{r}) \simeq -\text{j}k\eta\int_{S_a} \bar{\boldsymbol{G}}(\boldsymbol{r}, \boldsymbol{r}') \cdot \boldsymbol{J}^s(\boldsymbol{r}')\text{d}s' + \int_{S_a} \boldsymbol{M}^s(\boldsymbol{r}') \times \nabla G(\boldsymbol{r}, \boldsymbol{r}')\text{d}s' \tag{14}$$

where $\boldsymbol{J}^s(\boldsymbol{r}) = \boldsymbol{H}^s(\boldsymbol{r}) \times (-\hat{\boldsymbol{n}}(\boldsymbol{r}))$ and $\boldsymbol{M}^s(\boldsymbol{r}) = (-\hat{\boldsymbol{n}}(\boldsymbol{r})) \times \boldsymbol{E}^s(\boldsymbol{r})$ are the equivalent electric and magnetic current at the aperture. $\boldsymbol{E}^s(\boldsymbol{r})$ and $\boldsymbol{H}^s(\boldsymbol{r})$ are the scattering field from $\boldsymbol{J}(\boldsymbol{r})$ and $\boldsymbol{M}(\boldsymbol{r})$

$$\boldsymbol{E}^s(\boldsymbol{r}) = -\text{j}k\eta\int_{S_c} \bar{\boldsymbol{G}}(\boldsymbol{r}, \boldsymbol{r}') \cdot \boldsymbol{J}(\boldsymbol{r}')\text{d}s' + \int_{S_c} \boldsymbol{M}(\boldsymbol{r}') \times \nabla G(\boldsymbol{r}, \boldsymbol{r}')\text{d}s' \tag{15}$$

$$\boldsymbol{H}^s(\boldsymbol{r}) = -\int_{S_c} \boldsymbol{J}(\boldsymbol{r}') \times \nabla G(\boldsymbol{r}, \boldsymbol{r}')\text{d}s' - \frac{\text{j}k}{\eta}\int_{S_c} \bar{\boldsymbol{G}}(\boldsymbol{r}, \boldsymbol{r}') \cdot \boldsymbol{M}(\boldsymbol{r}')\text{d}s' \tag{16}$$

Numerical results: The normalised monostatic RCS of cavities are computed on the computer with Intel Core i9-9900k CPU. The incident plane waves are $\boldsymbol{\theta}$-polarised for all examples.

First, in order to verify the correctness of our code, a 4λ × 4λ IBC cylindrical cavity is calculated and compared with the IPO solution [7]. The normalised surface impedance of all the interior walls is 0.0797−j0.0050 [7]. The wall and the aperture of the cavity are modelled by 5451 RWG basis functions and 771 triangles, respectively. Fig. 2 shows the calculated RCS by our code and the IPO in [7]. It is apparent that the results are consistent.

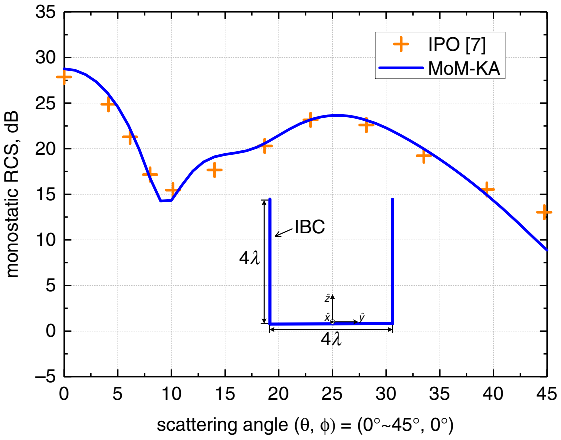

Fig. 2 *Monostatic RCS of* 4λ × 4λ *IBC cylindrical cavity*

Next, the monostatic RCS of a cavity with an IBC wall is simulated. The shape of the cavity is shown in Fig. 3, and it is obtained by the Boolean subtraction of two rectangular cavities: 6λ × 4λ × 8λ and 2λ × 4λ × 2λ. The area of the IBC wall is 2λ × 4λ. The normalised surface impedance η_r of the IBC wall is set to different values: 0.0, 0.2, 0.4, 0.6, 0.8. It should be noted that the IBC wall is equivalent to a PEC wall if $\eta_r = 0.0$. The aperture is discretised into 1334 triangles, all cavity walls are modelled by 14,923 RWG and the IBC wall contains 669 RWG. Fig. 3 shows the RCS results of this simulation computed by the proposed method and the conventional MoM-KA. It can be seen that the results are in good agreement. Table 1 compares the CPU time of the proposed method and the conventional MoM-KA. The two methods take the same time to calculate the voltage and impedance matrices, and to solve the cavity without IBC walls $(\eta_r = 0.0)$. However, the CPU time for solving the cavity with different IBC walls is cut down 82% by the proposed method.

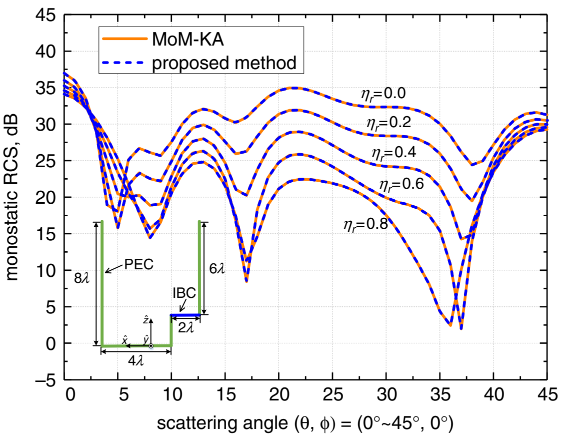

Fig. 3 *Monostatic RCS of cavity with IBC wall and normalised surface impedance has different values*

Table 1: Comparison of CPU time of different methods

	MoM-KA	Prop. method
generation of voltage and impedance matrix	127 s	
solution of PEC cavity $(\eta_r = 0.0)$	78 s	
solution of cavity with different IBC walls	353 s	63 s

Conclusion: An efficient method is presented to predict the interior scattering from a PEC cavity with different and small IBC walls. The method uses MFIE with KA [1–3] to estimate the cavity interior scattering, and uses the SMW formula [8–10] to avoid the repeated and expansive LU decompositions when the IBC wall is modified multiple times. Numerical results show that the method can save considerable amount of CPU time compared with the conventional MoM.

Acknowledgments: This work was supported by the National Nature Science Foundation of China (61771238, 61501227), the Postdoctoral Science Foundation of China (2017T100364), the Jiangsu Key Laboratory of Meteorological Observation and Information Processing Open Project (KDXS1802), the Joint Open Project of KLME & CIC-FEMD, NUIST (KLME201910), and the Foundation of State Key Laboratory of Millimeter Waves, Southeast University, China (K202035).

Submitted: *03 May 2020* E-first: *30 June 2020*
doi: 10.1049/el.2020.1339
One or more of the Figures in this Letter are available in colour online.

Xinlei Chen (*Jiangsu Key Laboratory of Meteorological Observation and Information Processing, Nanjing University of Information Science and Technology, Nanjing, People's Republic of China*)

✉ E-mail: chenxl@nuaa.edu.cn

Xiuqiang Liu, Zhuo Li and Changqing Gu (*College of Electronic and Information Engineering, Nanjing University of Aeronautics and Astronautics, People's Republic of China*)

Xinlei Chen: Also with Collaborative Innovation Center of Atmospheric Environment and Equipment Technology, Nanjing University of Information Science and Technology, Nanjing, People's Republic of China; College of Electronic and Information Engineering, Nanjing University of Aeronautics and Astronautics, People's Republic of China; KLME & CIC-FEMD, NUIST, People's Republic of China, and State Key Laboratory of Millimeter Waves, Southest University, People's Republic of China

References

1 Obelleiro-Basteiro, F., Rodriguez, J.L., and Burkholder, R.J.: 'An iterative physical optics approach for analysing the electromagnetic scattering by large open-ended cavities', *IEEE Trans. Antennas Propag.*, 1995, **43**, (4), pp. 356–361
2 Xiang, Z., and Chia, T.-T.: 'A hybrid BEM/WTM approach for analysis of the EM scattering from large open-ended cavities', *IEEE Trans. Antennas Propag.*, 2001, **49**, (2), pp. 165–173
3 Chen, X., Liu, X., and Gu, C.: 'Efficient calculation of interior scattering from cavities with small modifications', *Electron. Lett.*, 2020, **56**, (2), pp. 80–82
4 Altintas, A., Pathak, P.H., and Liang, M.C.: 'A selective modal scheme for the analysis of EM coupling into or radiation from large open-ended waveguides', *IEEE Trans. Antennas Propag.*, 1988, **36**, (1), pp. 84–96
5 Senior, T.B.A.: 'Impedance boundary conditions for imperfectly conducting surfaces', *Appl. Sci. Res., Section B.*, 1960, **8**, pp. 418–436
6 Obelleiro, F., Araujo, M.G., and Rodriguez, J.L.: 'Iterative physical-optics formulation for analyzing large waveguides with lossy walls', *IEEE Micro. Opt. Tech. Lett.*, 2001, **28**, (1), pp. 21–26
7 Tadokoro, M., and Hongo, K.: 'Measurement of RCS from a dielectric coated cylindrical cavity and calculation using IPO-EIBC', *IEICE Trans. Electron.*, 2002, **85**, (9), pp. 1692–1696
8 Yip, E., and Tomas, B.: 'Obtaining scattering solution for perturbed geometries and materials from moment method solutions', *ACES J.*, 1988, **3**, (2), pp. 95–118
9 Boag, A., Boag, A., Michielssen, E., *et al.*: 'Design of electrically loaded wire antennas using genetic algorithms', *IEEE Trans. Antennas Propag.*, 1996, **44**, (5), pp. 687–695
10 Hager, W.: 'Updating the inverse of a matrix', *SIAM Rev.*, 1989, **31**, (2), pp. 221–239
11 Nie, Z., Wang, H., and Wang, J.: 'A combined field solution with single operator for electromagnetic scattering from conductive targets with open cavities', *IEEE Trans. Antennas Propag.*, 2008, **56**, (6), pp. 1734–1741